

# Maximum mass of a hybrid star having a mixed-phase region based on constraints set by the pulsar PSR J1614-2230

Ritam Mallick\*

*Institute of Physics, Sachivalaya Marg, Bhubaneswar 751005, India*

(Received 15 October 2012; revised manuscript received 15 December 2012; published 19 February 2013)

Recent observation of pulsar PSR J1614-2230 with a mass of about two solar masses poses a severe constraint on the equations of state (EOSs) of matter describing stars under extreme conditions. Neutron stars (NSs) can reach the mass limit set by PSR J1614-2230, but stars having hyperons or quark stars (Qs) having boson condensates, with softer EOSs, can barely reach such limit and are ruled out. Qs with pure strange matter cannot attain such high mass unless the effect of strong coupling constants or color superconductivity are considered. In this work I calculate the upper mass limit for a hybrid star (HS) having a quark-hadron mixed phase. The hadronic matter (having hyperons) EOS is described by relativistic mean field theory and the quark matter EOS is modeled according to the Massachusetts Institute of Technology bag model. The intermediate mixed phase is constructed using the Glendenning prescription. A HS with a mixed phase cannot reach the mass limit set by PSR J1614-2230 unless one assumes a density-dependent bag constant. However, for such case the mixed-phase region is small. The maximum mass of a mixed hybrid star obtained with such a mixed-phase region is  $2.01M_{\odot}$ . A stiffer hadronic EOS can raise the maximum mass of a mixed HS to  $2.1M_{\odot}$ .

DOI: [10.1103/PhysRevC.87.025804](https://doi.org/10.1103/PhysRevC.87.025804)

PACS number(s): 26.60.Kp, 21.65.Qr, 97.10.Cv, 97.10.Nf

## I. INTRODUCTION

Neutron stars (NSs) are gravitationally bound. Therefore, the precise measurement of mass and radius of a NS should provide a very fine probe for the equation of state (EOS) of dense matter. The first reasonable idea about the composition of compact star was that matter is at extremely high densities and is mainly composed of neutrons with small fractions of protons and electrons. Further theoretical developments and modern experimental results opened the window to other possibilities. The central core density of a NS is about 3–10 times that of the nuclear saturation density ( $n_0 \sim 0.15 \text{ fm}^{-3}$ ). At such high densities, the matter is likely to be in a deconfined and chirally restored quark phase [1].

The strange matter hypothesis was first proposed by Itoh and Bodemer [2,3] and then improved by Witten [4]. It states that matter at extreme density and/or temperature is composed of almost equal numbers of up, down, and strange quarks known as strange quark matter (SQM). This is also said to be the ground state of strongly interacting matter at extreme conditions. If this is true, then the matter at extreme conditions is likely to eventually convert to SQM. Such a high-density scenario is present in the interior of a NS, and therefore normal nuclear matter is likely to undergo a phase transition to SQM. The strange matter hypothesis was first extensively studied in the simple Massachusetts Institute of Technology (MIT) bag model by Farhi and Jaffe [5]. The conversion process and the phase transition was further analyzed by Alcock *et al.* [6]. The phase transition in a NS may continue up to the surface of the star or may stop inside the star. Depending upon the region to which the quark matter extends, a quark star (QS) may be of two types, a strange star (SS) or a hybrid star (HS). SS are stars composed only of SQM, while HS has a quark core surrounded

by hadronic matter. In the region between the quark core and hadronic matter, there may exist a mixed-phase region where both quarks and hadrons are present.

Recently, Demorest *et al.* [7] found a new maximum mass limit for compact stars by measuring very precisely the mass of the millisecond pulsar PSR J1614-2230,  $1.97 \pm 0.04 M_{\odot}$ . This value is much higher than any previously measured pulsar mass. This measurement has imposed very severe constraints on the EOS of matter describing compact objects. NS models without hyperons can easily satisfy the new mass limit. However, the presence of strangeness, either in the form of hyperons in nuclear matter or strange quarks in quark matter, makes the EOS softer. Therefore, hadronic stars with hyperons and quark stars cannot easily satisfy the mass limit. Studies are being carried out to make the hyperonic and quark EOS satisfactorily explain the new mass constraint.

To satisfy the new mass limit, one has to make the EOS stiffer, which usually is softened by the presence of strangeness. However, recent studies have suggested that the stiffening of hyperonic EOS is possible even with the new experimental results [8]. Some authors also have revisited the role of vector meson-hyperon coupling [9] and hyperon potentials [10] to calculate the maximum mass.

In the quark sector, studies prior to the discovery of pulsar PSR J1614-2230 have suggested the stiffening of quark matter EOS from the effect of strong interactions, such as one-gluon exchange or color superconductivity [11–17]. Ozel [18] and Lattimer [19] studied the implications of the new mass limits from PSR J1614-2230 for quark and hybrid stars in the quark bag model. Recently, Bonanno and Sedrakian [20] succeeded in obtaining massive HSs. They employed a color-superconducting quark core and very stiff hadronic EOS (like the NL3 hyperonic model or the GM3 nuclear model) in their calculation.

In this work I perform an extensive study of HS mass. For the hadronic EOS I use the relativistic mean-field model and

\* ritam.mallick5@gmail.com

the quark EOS is described by three-flavor MIT bag model. I assume that the HS has a mixed phase in the intermediate region. The paper is organized as follows: In Sec. II, I describe the hadronic EOS, and in Sec. III, I describe the quark MIT bag model. The mixed-phase EOS is constructed in Sec. IV using the Glendenning prescription. I present my results in Sec. V. The maximum mass for the HS is calculated in this section. Finally in Sec. VI, I summarize my results and draw conclusions from them.

## II. HADRONIC PHASE

The matter at the outer region of the star is mainly composed of hadrons. I use the nonlinear relativistic mean field (RMF) model with hyperons (TM1 parametrization) to describe the hadronic phase EOS. In this model the baryons interact with mean meson fields [21–25].

The model Lagrangian density includes nucleons, baryon octet ( $\Lambda$ ,  $\Sigma^{0,\pm}$ ,  $\Xi^{0,-}$ ), and leptons:

$$\begin{aligned} \mathcal{L}_H = & \sum_b \bar{\psi}_b \left[ \gamma_\mu \left( i \partial^\mu - g_{\omega b} \omega^\mu - \frac{1}{2} g_{\rho b} \vec{\tau} \cdot \vec{\rho}^\mu \right) \right. \\ & - (m_b - g_{\sigma b} \sigma) \left. \right] \psi_b + \frac{1}{2} (\partial_\mu \sigma \partial^\mu \sigma - m_\sigma^2 \sigma^2) \\ & - \frac{1}{4} \omega_{\mu\nu} \omega^{\mu\nu} + \frac{1}{2} m_\omega^2 \omega_\mu \omega^\mu - \frac{1}{4} \vec{\rho}_{\mu\nu} \cdot \vec{\rho}^{\mu\nu} + \frac{1}{2} m_\rho^2 \vec{\rho}_\mu \cdot \vec{\rho}^\mu \\ & - \frac{1}{3} b m_n (g_\sigma \sigma)^3 - \frac{1}{4} c (g_\sigma \sigma)^4 + \frac{1}{4} d (\omega_\mu \omega^\mu)^2 \\ & + \sum_l \bar{\psi}_l [i \gamma_\mu \partial^\mu - m_l] \psi_l. \end{aligned} \quad (1)$$

Leptons  $l$  are noninteracting, but the baryons  $b$  are coupled with the scalar  $\sigma$  mesons, the isoscalar-vector  $\omega_\mu$  mesons, and the isovector-vector  $\rho_\mu$  mesons. The model constants are fitted in accordance with the experimental results from the bulk properties of nuclear matter [22,25]. The TM1 model satisfactorily explains the nuclear saturation but cannot model the hyperonic matter sufficiently, as it fails to reproduce the strong observed  $\Lambda\Lambda$  attraction. This defect was remedied by Mishustin and Schaffner [25] by the addition of isoscalar scalar  $\sigma^*$  mesons and the isovector vector  $\phi$  mesons, which couple only with the hyperons. I denote this model by TM1L.

The detailed EOS calculation can be found in Refs. [24,25], and I do not repeat them here. The TM1L model generates a relatively soft EOS. For completeness, I compare the maximum mass of the HS obtained from the TM1L model with the maximum mass of the HS obtained from a much stiffer EOS, known as the PL-Z model [25,26]. In Table I, I give the different coupling constants for the two parametrizations.

For the models, the total energy density takes the form

$$\begin{aligned} \varepsilon = & \frac{1}{2} m_\omega^2 \omega_0^2 + \frac{1}{2} m_\rho^2 \rho_0^2 + \frac{1}{2} m_\sigma^2 \sigma^2 + \frac{1}{2} m_{\sigma^*}^2 \sigma^{*2} \\ & + \frac{1}{2} m_\phi^2 \phi_0^2 + \frac{3}{4} d \omega_0^4 + U(\sigma) + \sum_b \varepsilon_b + \sum_l \varepsilon_l, \end{aligned} \quad (2)$$

and the pressure can be represented as

$$P = \sum_i \mu_i n_i - \varepsilon, \quad (3)$$

TABLE I. Table showing the coupling constants for the two different parametrization used in the calculation. The nucleons do not couple with  $\sigma^*$  and  $\phi$ . The  $\Lambda$  does not couple with isovector field ( $g_{\rho\Lambda} = 0$ ). The coupling constant for  $\sigma$  is the same as that of  $\Lambda$  except for the isovector coupling ( $g_{\rho\Sigma} = 2g_{\rho N}$ ).

Coupling	PL-Z	TM1L
$g_{\sigma N}$	10.4262	10.0289
$g_{\omega N}$	13.3415	12.6139
$g_{\rho N}$	4.5592	4.6322
$g_{\sigma\Lambda}$	6.41	6.21
$g_{\omega\Lambda}$	8.89	8.41
$g_{\sigma^*\Lambda}$	6.93	6.67
$g_{\phi\Lambda}$	-6.29	-5.95
$g_{\sigma\Sigma}$	3.52	3.49
$g_{\omega\Sigma}$	4.45	4.20
$g_{\rho\Sigma}$	4.56	4.63
$g_{\sigma^*\Sigma}$	12.95	12.35
$g_{\phi\Sigma}$	-12.58	-11.89

where  $\mu_i$  and  $n_i$  are the chemical potential and number density of particle species  $i = b, l$ .

## III. QUARK PHASE

The quark phase is modeled according to the simple MIT bag model [27]. The current masses of up and down quarks are extremely small and are assumed to be 5 and 10 MeV, respectively. The strange quark current quark mass is not well established, and I vary it in my calculation. For the bag model the energy density and the pressure are given by

$$\epsilon^Q = \sum_{i=u,d,s} \frac{g_i}{2\pi^2} \int_0^{k_F^i} dk k^2 \sqrt{m_i^2 + k^2} + B_G, \quad (4)$$

$$P^Q = \sum_{i=u,d,s} \frac{g_i}{6\pi^2} \int_0^{k_F^i} dk \frac{k^4}{\sqrt{m_i^2 + k^2}} - B_G, \quad (5)$$

where  $k_F^i = \sqrt{\mu_i^2 - m_i^2}$  and  $g_i$  is the Fermi momentum and degeneracy factor of quark species  $i$ .  $B_G$  is the energy density difference between the perturbative vacuum and the true vacuum, i.e., the bag constant.  $B_G$  is considered a free parameter in my calculation.

Both the hadronic and quark matter maintain baryon number conservation. They are charge neutral and in  $\beta$  equilibrium.

## IV. MIXED PHASE

With the described hadronic and quark EOS, Glendenning prescription [28] gives the mixed-phase regime. The mixed phase is the baryon density range where both quarks and hadrons are present. In the mixed phase the hadron and the quark phases are separately charged but the mixed phase is charge neutral as a whole. The matter can be parametrized by the pair of electron and baryon chemical potentials  $\mu_e$

and  $\mu_n$ . Pressure of the two phases are made equal to maintain mechanical equilibrium. To satisfy the chemical and  $\beta$  equilibrium conditions, the chemical potential of different particles are related to each other. The Gibbs criterion gives the mechanical and chemical equilibrium between two phases and is given by

$$P_{\text{HP}}(\mu_e, \mu_n) = P_{\text{QP}}(\mu_e, \mu_n) = P_{\text{MP}}. \quad (6)$$

The solution of the above equation gives the equilibrium chemical potentials of the mixed phase. As the two phases intersect one can calculate the corresponding charge densities of the hadronic components  $\rho_c^{\text{HP}}$  and quark components  $\rho_c^{\text{QP}}$  separately in the mixed phase. The volume fraction occupied by quark matter  $\chi$  in the mixed phase is given by

$$\chi \rho_c^{\text{QP}} + (1 - \chi) \rho_c^{\text{HP}} = 0. \quad (7)$$

The mixed-phase energy density  $\epsilon_{\text{MP}}$  and the number density  $n_{\text{MP}}$  can be written as

$$\epsilon_{\text{MP}} = \chi \epsilon_{\text{QP}} + (1 - \chi) \epsilon_{\text{HP}}, \quad (8)$$

$$n_{\text{MP}} = \chi n_{\text{QP}} + (1 - \chi) n_{\text{HP}}. \quad (9)$$

Therefore, the EOS is now a system having a charge-neutral hadronic phase at lower densities, a charge-neutral mixed phase in the intermediate density region, and a charge-neutral quark phase at higher densities.

## V. RESULTS

The EOS governs the properties of a compact star. The central region of the star has maximum density (few times  $n_0$ ); therefore, the matter at the core is most likely to have a phase transition. The central region would therefore have stable strange matter (or a color-superconducting matter). As the density decreases radially outward hadronic matter starts appearing and so the intermediate region is likely to have a mixed phase. Much further outward matter consists of only hadrons. The crust consists mainly of free electrons and nuclei, which completes the star structure.

The hadronic EOS with the TM1L parameter set satisfactorily explains the properties of hadronic matter. Once the parametrization is chosen, the model is fixed. One can control the quark EOS by changing the strange quark mass and the bag constant. The masses of the light quarks are quite bounded, and I assume them to be 5 MeV (u) and 10 MeV (d). The mass of the  $s$  quark is still not well established but is expected to be between 100 and 300 MeV. I vary the mass of the  $s$  quark within this mass range. I also vary the bag constant ( $B_G$ ) to regulate the mixed phase. This parametrization of the EOS of the hadron and quark matter is responsible for characterization of the matter in the mixed phase. Using the Glendenning prescription to construct the mixed phase, I plot curves of pressure against energy density in Fig. 1. The figure shows curves for the mixed-phase EOS with bag pressures 170 and 180 MeV. Actually the relation runs as  $B_G^{1/4} = 170$  MeV, but for simplicity I denote  $B_G^{1/4} = 170$  MeV =  $B_g$ . For this case the mass of the  $s$  quark ( $m_s$ ) is taken to be 150 MeV. With constant bag pressure, bag pressure lower than 170 MeV cannot generate a mixed-phase region. In the curves, the

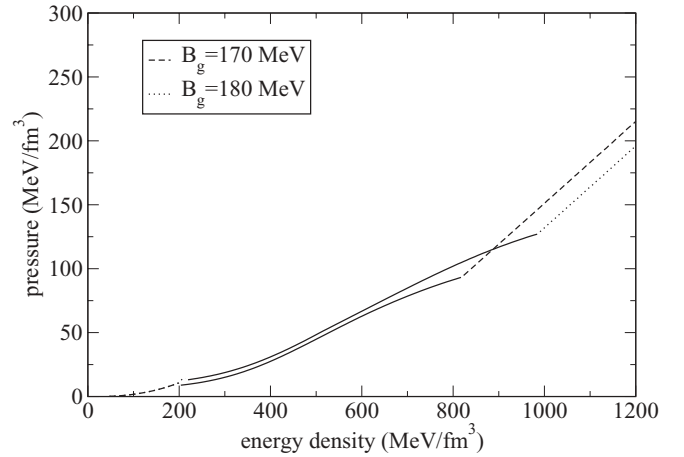


FIG. 1. Pressure as a function of energy density with bag pressures of 170 and 180 MeV.

lower portion is the nuclear phase (dotted/dashed line), the intermediate region is the mixed phase (bold line), and the higher region is the quark phase (dotted/dashed line). Figure 2 shows the pressure against baryon density for the EOSs with bag constants 170 and 180 MeV. The mixed phase starts at  $0.2 \text{ fm}^{-3}$  and ends at  $0.76 \text{ fm}^{-3}$  for bag pressure 170 MeV, whereas for bag pressure 180 MeV the mixed phase is between  $0.22$  and  $0.89 \text{ fm}^{-3}$ . The EOS curve with bag constant 170 MeV is much stiffer than the EOS curve with bag pressure 180 MeV, because the bag pressure adds negatively to the matter pressure, making the effective pressure low. The curves also show that as the bag pressure increases the mixed-phase region increases. The variation of pressure with energy density and baryon density are quite similar. Therefore, from now on I only plot the curve showing pressure as function of energy density.

With such high values of bag pressure it is impossible to attain the mass limit set by PSR J1614-2230. Therefore, to have a stiffer EOS I assume density-dependent bag pressure.

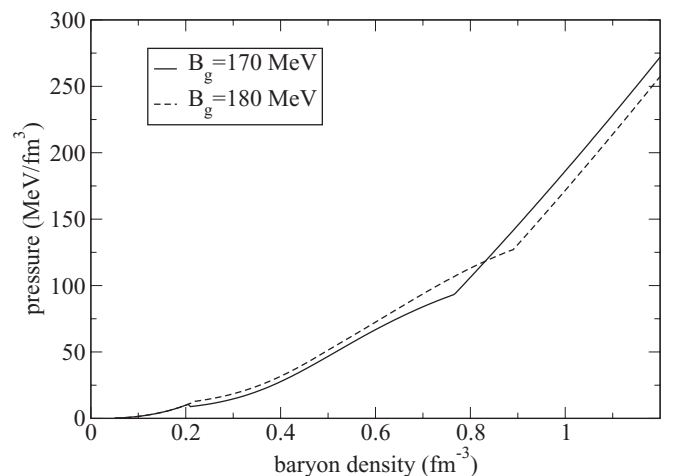


FIG. 2. Pressure as a function of baryon density with bag pressures of 170 and 180 MeV.

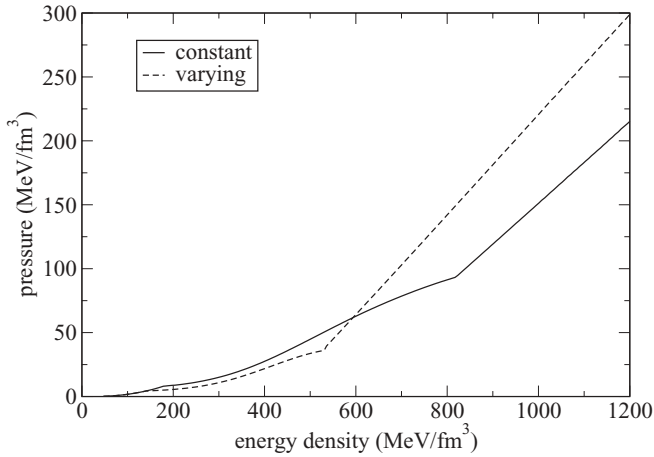


FIG. 3. Pressure against energy density plot with constant and varying bag pressure, having  $B_g = 170$  MeV.

In the literature there are several attempts to understand the density dependence of  $B_g$  [29,30]; however, currently the results are highly model dependent. I parametrized the bag constant in such a way that it attains a value  $B_\infty$ , asymptotically at high densities. The range of value of  $B_\infty$  obtained from experiments can be found in Burgio *et al.* [31], and I assume it to be 130 MeV, the lowest value mentioned there. With such assumptions I vary the bag pressure with baryon density according to a Gaussian parametrization, which is given by [31,32]

$$B_{gn}(n_b) = B_\infty + (B_g - B_\infty) \exp \left[ -\beta \left( \frac{n_b}{n_0} \right)^2 \right]. \quad (10)$$

The lowest value of  $B_{gn}$ , which is its value at asymptotic high density in quark matter, is fixed at 130 MeV. The bag pressure quoted from now on would be the value of the bag pressure at the beginning of the mixed-phase region ( $B_g$  in the equation). As the density increases the bag pressure decreases and reaches 130 MeV asymptotically; the decrease rate is controlled by  $\beta$ .

In Fig. 3 I have plotted curves with and without the variation of bag pressure (for  $B_g = 170$  MeV). The figure shows that the EOS with varying bag pressure is much stiffer than the EOS with constant bag pressure. For the varying bag pressure the mixed-phase region shrinks and becomes flatter, but the quark phase becomes stiffer. The mixed-phase region extends only up to baryon density of  $0.53 \text{ fm}^{-3}$ . The change in the mixed-phase region is about  $\sim 30\%$ . The curve becomes stiff toward higher densities (or higher energy density) because the effective matter pressure increases with the decrease in bag pressure (bag pressure adds negatively to the matter pressure). With such a density-dependent bag constant one can have a mixed-phase region with lower values of bag pressure. As shown in Fig. 4 one can have a mixed-phase region with bag pressures of 160 and 150 MeV. EOS with  $B_g = 160$  MeV have  $s$ -quark mass ( $m_s$ ) of 150 MeV, and for EOS with  $B_g = 150$  MeV the  $s$ -quark mass is 300 MeV. With  $B_g = 160$  and  $B_g = 150$  MeV the mixed-phase region is considerably small. For  $B_g = 160$  MeV the mixed-phase

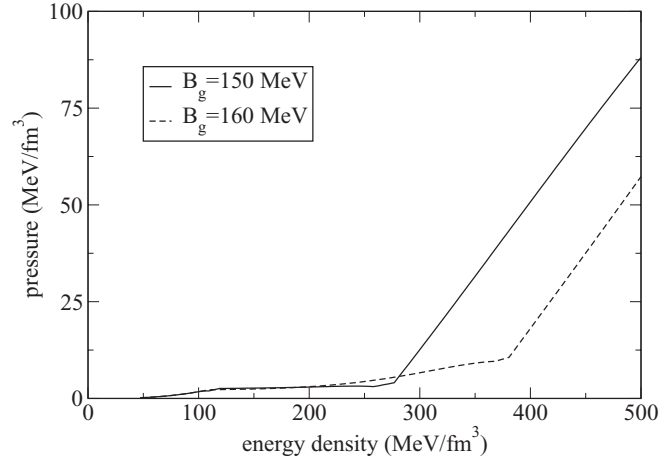


FIG. 4. Pressure against energy density plot with varying bag pressure, having  $B_g = 160$  and  $150$  MeV.

region starts at  $0.15 \text{ fm}^{-3}$  baryon density and ends at  $0.36 \text{ fm}^{-3}$  baryon density. For EOS with  $B_g = 150$  MeV the mixed phase starts at  $0.13 \text{ fm}^{-3}$  baryon density and ends at  $0.3 \text{ fm}^{-3}$  baryon density. In Fig. 5 I have separately plotted the EOS for  $B_g = 150$  MeV showing the mixed phase region clearly. As shown later, with such choice of quark matter parameters (bag constant and strange quark mass) one can attain the mass limit set by PSR J1614-2230. For this the value of  $\beta$  is 0.0035. This is the maximum value of  $\beta$  for which one gets a finite mixed-phase region. For higher value of  $\beta$  the mixed phase disappears.  $\beta$  is the parameter that decides how fast the bag constant falls to its lowest asymptotic value of 130 MeV. As the value of  $\beta$  becomes greater, it falls faster. In Fig. 6 I have shown the variation of bag pressure with energy density for three  $\beta$  values, 0.001, 0.002, and 0.0035. I find that as the value of  $\beta$  increases, the rate of fall of bag pressure increases. In Fig. 7 I have shown the variation of pressure against energy density for the same three  $\beta$  values, with  $B_g = 150$  MeV. I find that as  $\beta$  increases the EOS

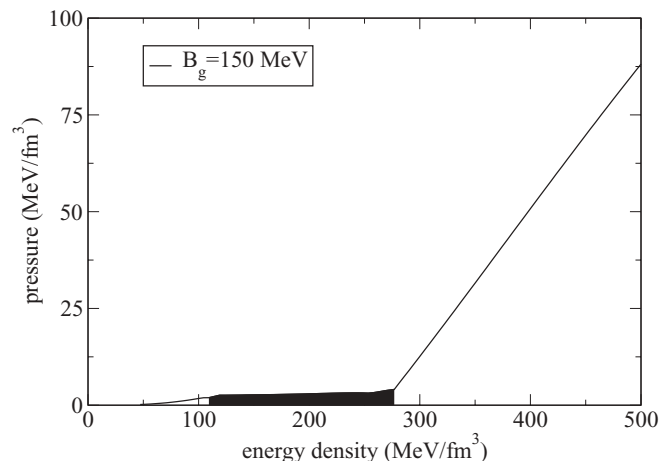


FIG. 5. Pressure against energy density plot showing explicitly the mixed-phase region, for the varying bag pressure  $B_g = 150$  MeV.

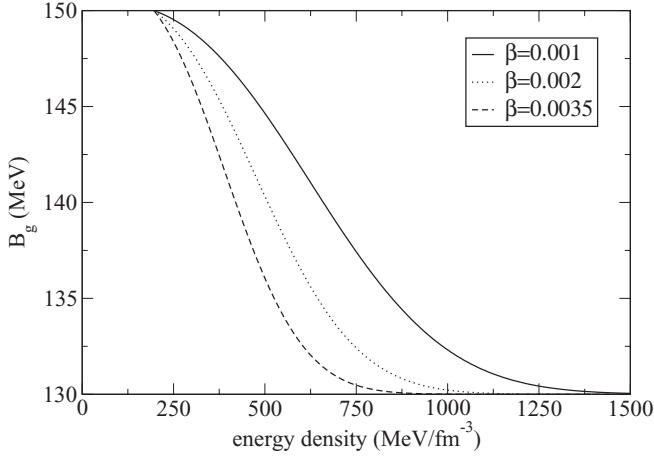


FIG. 6. Bag pressure against energy density curves for three values of  $\beta$ : 0.001, 0.002, and 0.0035.

becomes stiffer, with all other bag parameters remaining the same.

I should mention here that the Bodmer-Witten conjecture is valid for the MIT bag model for a certain “stability window.” If the three-flavor quark matter is the absolute stable ground state, then at zero pressure, the energy density per baryon for the three-flavor matter has to be lower than that for iron, which is 930 MeV. Therefore, for my analysis I can do a simple calculation to see the value of energy per baryon. With the given quark masses mentioned previously, for  $B_g = 180$  MeV and  $B_g = 170$  MeV, the energies per baryon are 963 and 942 MeV respectively. Therefore, for such choices the quark matter is not stable. For  $B_g = 160$  MeV the value is 911 MeV, which makes the quark matter stable for varying bag pressure of 160 MeV. For  $B_g = 150$  MeV the value is 920 MeV. The value of the energy per baryon for  $B_g = 150$  MeV is greater than that of  $B_g = 160$  MeV because for  $B_g = 150$  MeV the  $s$ -quark mass is 300 MeV, whereas for  $B_g = 160$  MeV the  $s$ -quark mass is 150 MeV. For the same value of  $s$ -quark mass, the energy per baryon

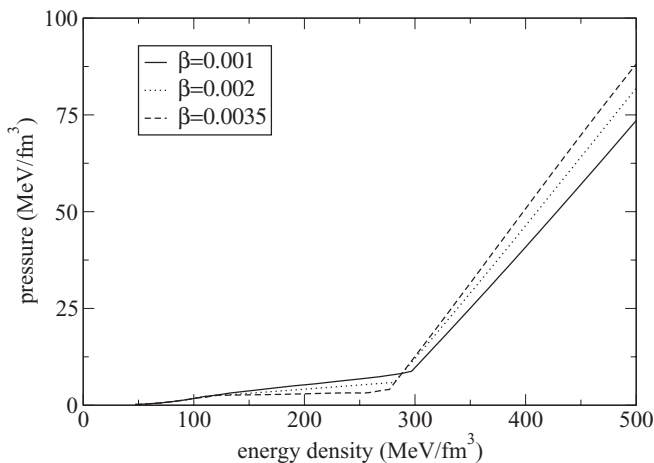


FIG. 7. Pressure against energy density curves for three values of  $\beta$ : 0.001, 0.002, and 0.0035, with  $B_g = 150$  MeV.

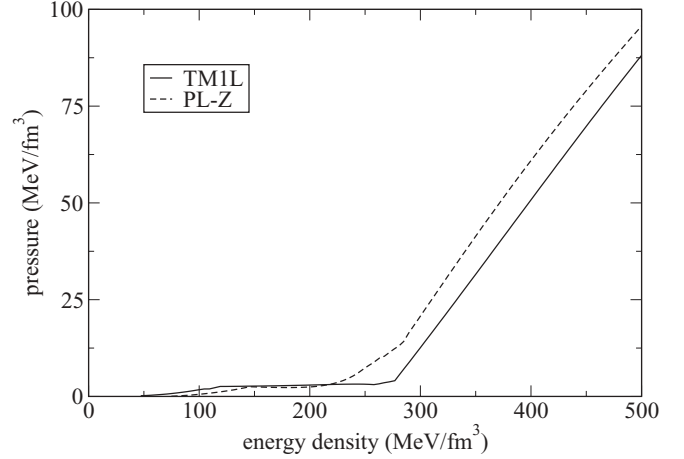


FIG. 8. Pressure against energy density plot showing the mixed-phase region for the varying bag pressure  $B_g = 150$  MeV for TM1L and PL-Z EOSs.

for  $B_g = 150$  MeV is lower than  $B_g = 160$  MeV. However, to have the maximum mass of a hybrid star the quark matter is stable.

As mentioned previously, for completeness, I construct the mixed EOS with the PL-Z hadronic model. In Fig. 8 I plot the PL-Z and TM1L EOSs for comparison. The hadronic PL-Z EOS is much stiffer than the TM1L EOS. However, in the mixed phase the stiffness is not very large as the hadronic EOS affects only the low-density region of the mixed EOS curve.

Assuming the star to be stationary and spherical, the Tolman-Oppenheimer-Volkoff (TOV) equations [33] give the solution for the pressure  $P$  and the enclosed mass  $m$ ,

$$\frac{dP(r)}{dr} = -\frac{Gm(r)\epsilon(r)}{r^2} \frac{[1+P(r)/\epsilon(r)][1+4\pi r^3 P(r)/m(r)]}{1-2Gm(r)/r},$$

$$\frac{dm(r)}{dr} = 4\pi r^2 \epsilon(r), \quad (12)$$

with  $G$  being the gravitational constant. Starting with a fixed central energy density  $\epsilon(r=0) \equiv \epsilon_c$ , I integrate radially outward until the pressure on the surface equals the one corresponding to the density of iron. This gives the star's radius  $R$  having gravitational mass

$$M_G \equiv m(R) = 4\pi \int_0^R dr r^2 \epsilon(r). \quad (13)$$

For the NS crust, in the medium-density range I add the hadronic EOS by Negele and Vautherin [34], and for the outer crust I add the EOS by Feynman *et al.* [35] and Baym *et al.* [36].

Figure 9 shows the gravitational mass  $M$  (in units of solar mass  $M_\odot$ ) as a function of radius  $R$ , for constant and varying bag pressure,  $B_g = 170$  MeV. A stiffer EOS generates a stiffer mass-radius curve. Therefore, the maximum mass of the star with varying bag pressure is higher than the nonvarying one. With such varying bag pressure I plot the mass-radius curve with  $B_g = 160$  MeV and 150 MeV (Fig. 10). With same qualitative aspect I find that the maximum mass of a mixed hybrid star obtained with  $B_g = 160$  MeV is  $1.84M_\odot$ . The

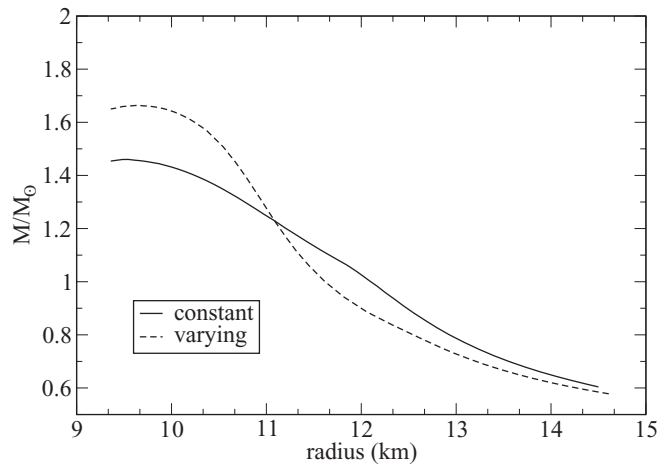


FIG. 9. Mass-radius curve with constant and varying bag pressure,  $B_g = 170$  MeV.

maximum mass with  $B_g = 150$  MeV and  $m_s = 300$  MeV is  $2.01 M_\odot$ .

The discovery of high-mass pulsar PSR J1614-2230 [7], with mass of about  $1.97 M_\odot$ , has set a stringent condition on the EOSs describing the interior of a compact star. The authors [7] quote the typical values of the central density of J1614-2230, for the allowed EOSs are in the range of  $2n_0$ – $5n_0$ , whereas consideration of the EOS-independent analysis [37] sets the upper central density limit at  $10n_0$ . With our prescription, the maximum mass of a mixed HS with  $m_s = 150$  MeV is found to be  $1.84 M_\odot$ . The maximum mass for the mixed HS can be increased to  $2.01 M_\odot$ , with  $m_s = 300$  MeV and having a varying bag pressure of  $B_g = 150$  MeV. Such choice of the quark matter parametrization can give rise to a mixed HS which would satisfy the mass limit set by PSR J1614-2230. However, with such choice of parameters the mixed-phase region is small.

It should be mentioned here that I have taken only the Gibbs condition for the HS. This choice ensures a mixed-phase region

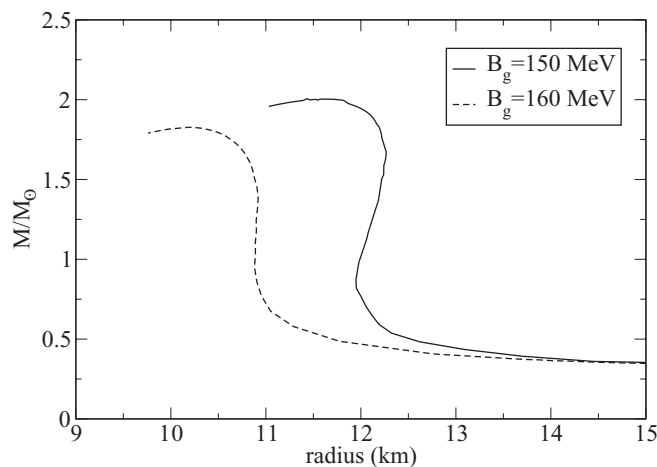


FIG. 10. Mass-radius curve with varying bag pressures,  $B_g = 160$  and  $150$  MeV.

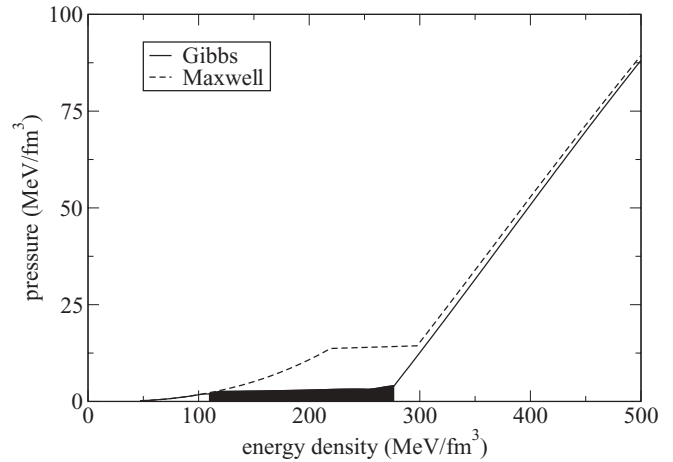


FIG. 11. Pressure against energy density plot for Gibbs and Maxwell construction of the mixed phase EOS.

and neglects the Coulomb and surface energies. There can be another extreme condition for HS, the Maxwell condition, corresponding to high surface tension of quark matter [38,39]. In such case the matter has a sudden jump transition from hadronic to quark phase. In Fig. 11 I have plotted the EOS curve for both the Gibbs and Maxwell approaches. For the Gibbs approach I find an extended mixed-phase region, whereas for the Maxwell approach there is a jump in the energy density (corresponding to a jump in density) from the lower hadronic to higher quark matter. In Fig. 12 I have shown the mass-radius relationship for the two approaches with my given formalism and EOS sets. I find that the maximum mass for the Maxwell approach is slightly higher,  $2.06 M_\odot$ .

As mentioned earlier, I also show the mass-radius curve for the mixed HS with stiffer hadronic EOS (PL-Z model) having the same quark matter parametrization ( $B_g = 150$  MeV and  $m_s = 300$  MeV). The maximum mass for the mixed HS attains a much higher value of  $2.1 M_\odot$  as shown in Fig. 13.

In this study I am mainly interested in studying the maximum mass of a mixed HS. The maximum mass of a

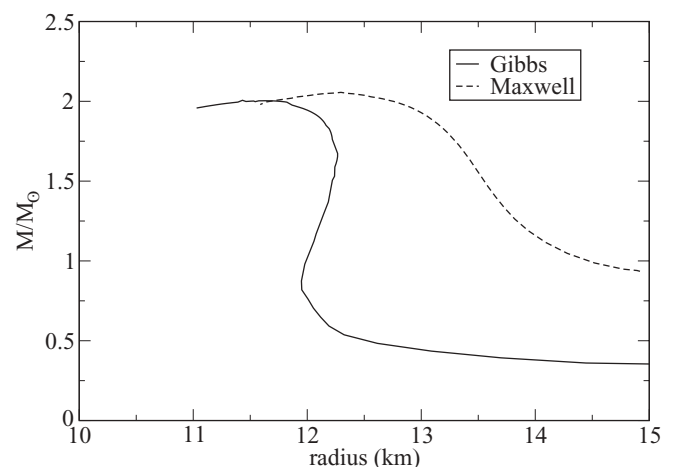


FIG. 12. Mass-radius curve for Gibbs and Maxwell construction of the HS.

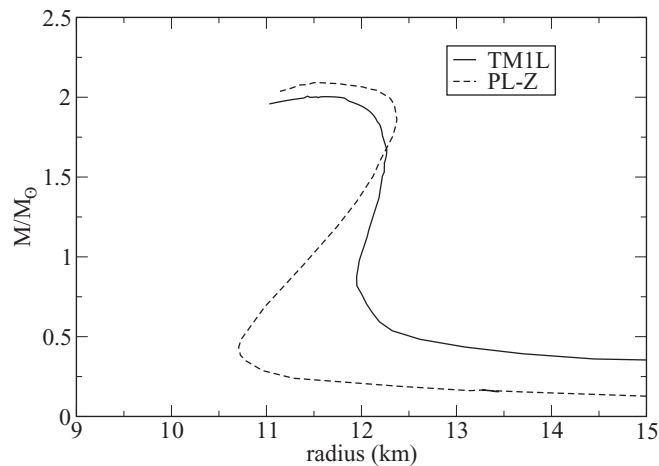


FIG. 13. Mass-radius curve with varying bag pressure, 150 MeV, for TMIL and PL-Z EOS.

HS with Gibbs approach is found to be  $2.01M_{\odot}$  and with Maxwell approach is  $2.06M_{\odot}$ . Stiffer EOS (PI-Z) takes the maximum mass of the mixed HS to a much higher value of  $2.1M_{\odot}$ . Nonhyperonic hadronic EOS could generate higher masses for HS [9]. Stiffer EOS sets (like hadronic NL3 and quark quark NJL model) for the mixed hybrid star can produce a much higher mass limit [40]. However, the aim of this paper was to see if a simple soft hyperonic and quark matter EOS can generate a HS which satisfies the mass limit set by the pulsar PSR J1614-2230. I have used a simple quark matter EOS, the MIT bag model, and by varying the bag pressure one can successfully maintain the mass limit set by PSR J1614-2230. It should be mentioned that in compact stars at high densities (mostly in their cores) there may be pairing of up, down, and strange quarks to form the so-called color-flavor locked (CFL) superconducting phase [41]. Such an exotic phase in the interiors of the stars produces stable HS masses which are quite high (much beyond  $2M_{\odot}$ ) [9,20]. In my calculation I have not used such CFL superconducting phase, but it is likely that such an exotic phase in quark matter would push the limit of the maximum mass to higher values.

From the mass-radius figures it is also clear that the maximum mass of the star corresponds to a radius of around 10 km. Therefore, the mixed hybrid star has a radius, corresponding to the maximum mass, in between neutron and strange stars. However, in a recent calculation by Paoli and Menezes [43], they showed that it may not always be the case. There they used NJL model to describe the quark phase and reached the conclusion that the mass-radius value of a compact star depends on the choice of the EOS model (both hadronic and quark).

## VI. SUMMARY AND CONCLUSION

In this work I have studied the maximum mass of a hybrid star having a mixed-phase region. With a relatively soft hadronic matter EOS having hyperons, and remaining in the simple MIT bag model, I wanted to study what parameter values could generate a massive HS having a mixed-phase

region. The HS has a dense quark core, a mixed intermediate phase, and hadronic outer region. The mixed phase is determined in accordance with the Glendenning prescription. All the phases are at chemical and mechanical equilibrium and are charge neutral as a whole. With constant bag pressures  $B_g = 170$  and  $B_g = 180$  MeV (and  $m_s = 150$  MeV) I get an EOS having a considerable mixed-phase region, but with such parametrization the maximum mass of the star is about  $1.5M_{\odot}$ . Also a simple analysis finds that for such choice of bag pressure values the SQM is not absolutely stable. I therefore consider a density-dependent bag pressure  $B_g$ , parametrized according to the Gaussian parametrization. The asymptotic value of the bag constant at high density is fixed at 130 MeV, which is its lowest value known from the experiments [31]. With such varying bag pressure I can have a mixed phase region with  $B_g = 160$  MeV, but still the mass of the star is below  $1.9M_{\odot}$ . To reach the mass limit set by PSR J1614-2230, one has to build the mixed EOS with bag pressure of  $B_g = 150$  MeV, having  $s$ -quark mass  $m_s = 300$  MeV and  $\beta = 0.0035$ . However, for such choice of parameter values the mixed-phase region is small. Further lowering of bag pressure is not possible, as then the mixed phase disappears. The maximum mass for a mixed hybrid star with the given sets of parameter values is found to be  $2.01M_{\odot}$ . A stiffer hadronic EOS takes the maximum mass to  $2.1M_{\odot}$ . If one has a direct jump from the hadronic to quark matter, the Maxwell approach, the maximum mass of the HS is  $2.06M_{\odot}$ .

After the discovery of PSR J1614-2230, setting the mass limit of compact stars to be  $2M_{\odot}$ , new EOS models are being proposed. Weissenborn *et al.* [42] showed that an absolutely stable strange star can have a mass above  $2$  *et al* if the effect of strong coupling constant and color superconductivity is taken into account. Bednarek *et al.* [8] argued that EOS with hyperons having quartic terms involving hidden strange vector mesons can reach such a high mass limit. Matsuda *et al.* [44] extended their calculation to hybrid stars, having a smooth crossover from hadronic to quark matter. For the star to reach the maximum mass limit they showed that the crossover has to take place at low density and the quark matter has to be strongly interacting. Using very stiff EOS sets (hadronic NL3 and quark quark NJL model), the maximum mass limit for the hybrid star can be raised to much higher values as shown by Lenzi and Lugones [40]. In my work, I have shown that the maximum mass limit can be attained by a HS with a mixed phase even with a relatively soft hadronic matter EOS having hyperons and the MIT bag model quark matter EOS, if one assumes a relatively low density-dependent bag pressure.

Observationally the NSs are characterized only by the signals coming to us from their surface. Developments had been made to accurately measure the mass of a compact star, but the same cannot be done for its radius. Reasonable measurement of the radius of a compact star could differentiate NSs, SSs, and HSs, as different EOSs of matter give different mass-radius relationships. Recent calculations show that by tuning parameter values or invoking new terms in the EOS analysis, the mass limit set by PSR J1614-2230 can be attained. Therefore, to have a full understanding of the matter at extreme densities we need results not only from astrophysical observations but also from earth-based experiments.

- [1] F. Weber, *Pulsars as Astrophysical Laboratories for Nuclear and Particle Physics* (IOP Publishing, Bristol, 1999).
- [2] N. Itoh, *Prog. Theor. Phys.* **44**, 291 (1970).
- [3] A. R. Bodmer, *Phys. Rev. D* **4**, 1601 (1971).
- [4] E. Witten, *Phys. Rev. D* **30**, 272 (1984).
- [5] E. Farhi and R. L. Jaffe, *Phys. Rev. D* **30**, 2379 (1984).
- [6] C. Alcock, E. Farhi, and A. Olinto, *Astrophys. J.* **310**, 261 (1986).
- [7] P. Demorest, T. Pennucci, S. Ransom, M. Roberts, and J. Hessels, *Nature (London)* **467**, 1081 (2010).
- [8] I. Bednarek, P. Haensel, J. L. Zdunik, M. Bejger, and R. Manka, [arXiv:1111.6942](https://arxiv.org/abs/1111.6942) [astro-ph.SR].
- [9] S. Weissenborn, D. Chatterjee, and J. Schaffner-Bielich, *Phys. Rev. C* **85**, 065802 (2012).
- [10] S. Weissenborn, D. Chatterjee, and J. Schaffner-Bielich, *Nucl. Phys. A* **881**, 62 (2012).
- [11] G. Lugones and J. E. Horvath, *Astron. Astrophys.* **403**, 173 (2003).
- [12] J. E. Horvath and G. Lugones, *Astron. Astrophys.* **442**, L1 (2004).
- [13] S. B. R uster and D. H. Rischke, *Phys. Rev. D* **69**, 045011 (2004).
- [14] M. Alford, D. Blaschke, A. Drago *et al.*, *Nature (London)* **445**, 7 (2007).
- [15] T. Fischer, I. Sagert, G. Pagliara *et al.*, *Astrophys. J. Supp.* **194**, 39 (2010).
- [16] A. Kurkela, P. Romatschke, and A. Vuorinen, *Phys. Rev. D* **81**, 105021 (2010).
- [17] A. Kurkela, P. Romatschke, A. Vuorinen, and B. Wu, [arXiv:1006.4062](https://arxiv.org/abs/1006.4062) [astro-ph.HE].
- [18] F.  zel, D. Psaltis, S. Ransom, P. Demorest, and M. Alford, *Astrophys. J. Lett.* **724**, L199 (2010).
- [19] J. M. Lattimer and M. Prakash, [arXiv:1012.3208](https://arxiv.org/abs/1012.3208) [astro-ph.SR].
- [20] L. Bonanno and A. Sedrakian, *Astron. Astrophys.* **539**, A16 (2012).
- [21] J. Boguta and R. A. Bodmer, *Nucl. Phys. A* **292**, 413 (1977).
- [22] N. K. Glendenning and S. A. Moszkowski, *Phys. Rev. Lett.* **67**, 2414 (1991).
- [23] S. K. Ghosh, S. C. Phatak, and P. K. Sahu, *Z. Phys. A* **352**, 457 (1995).
- [24] Y. Sugahara and H. Toki, *Nucl. Phys. A* **579**, 557 (1994).
- [25] J. Schaffner and I. N. Mishustin, *Phys. Rev. C* **53**, 1416 (1996).
- [26] P. G. Reinhard, *Z. Phys. A* **329**, 257 (1988).
- [27] A. Chodos, R. L. Jaffe, K. Johnson, C. B. Thorn, and V. F. Weisskopf, *Phys. Rev. D* **9**, 3471 (1974).
- [28] N. K. Glendenning, *Phys. Rev. D* **46**, 1274 (1992).
- [29] C. Adami and G. E. Brown, *Phys. Rep.* **234**, 1 (1993); X.-M. Jin and B. K. Jennings, *Phys. Rev. C* **55**, 1567 (1997).
- [30] D. Blaschke, H. Grigorian, G. Poghosyan, C. D. Roberts, and S. Schmidt, *Phys. Lett. B* **450**, 207 (1999).
- [31] G. F. Burgio, M. Baldo, P. K. Sahu, and H. J. Schulze, *Phys. Rev. C* **66**, 025802 (2002).
- [32] R. Mallick and P. K. Sahu, [arXiv:1207.4870](https://arxiv.org/abs/1207.4870) [astro-ph.HE].
- [33] S. L. Shapiro and S. A. Teukolsky, *Black Holes, White Dwarfs, and Neutron Stars* (John Wiley and Sons, New York, 1983).
- [34] J. W. Negele and D. Vautherin, *Nucl. Phys. A* **207**, 298 (1973).
- [35] R. Feynman, F. Metropolis, and E. Teller, *Phys. Rev.* **75**, 1561 (1949).
- [36] G. Baym, C. Pethick, and D. Sutherland, *Astrophys. J.* **170**, 299 (1971).
- [37] J. M. Lattimer and M. Prakash, *Phys. Rev. Lett.* **94**, 111101 (2005).
- [38] U. Seifert, *Phys. Rev. Lett.* **70**, 1335 (1993).
- [39] T. Endo, T. Maruyama, S. Chiba, and T. Tatsumi, *Prog. Theor. Phys.* **115**, 337 (2006).
- [40] C. H. Lenzi and G. Lugones, *Astrophys. J.* **759**, 57 (2012).
- [41] M. Alford, K. Rajagopal, S. Reddy, and F. Wilczek, *Phys. Rev. D* **4**, 074017 (2001).
- [42] S. Weissenborn, I. G. Sagert, M. Hempel, and J. Schaffner-Bielich, *Astrophys. J.* **740**, L14 (2011).
- [43] M. G. Paoli and D. P. Menezes, *Eur. Phys. J. A* **46**, 413 (2010).
- [44] K. Masuda, T. Hatsuda, and T. Takatsuka, [arXiv:1205.3621](https://arxiv.org/abs/1205.3621) [nucl-th].